J|A|C|S
COMMUNICATIONS

Published on Web 12/24/2002

Dynamic Effects on *J*-Couplings Across Hydrogen Bonds in Proteins

Phineus R. L. Markwick,* Remco Sprangers, and Michael Sattler*

European Molecular Biology Laboratory, Meyerhofstrasse 1, 69117 Heidelberg, Germany

Received October 9, 2002; E-mail: marwick@embl.de, sattler@embl.de

Hydrogen bonds are of fundamental importance in stabilizing biomolecular structure and play a key role in nearly all enzymatic reactions.[1] The recent observation of large *J*-couplings across hydrogen bonds by NMR[2] has prompted considerable experimental[3] and theoretical research[4] in this field due to the potential that these couplings hold for the determination of secondary and tertiary structure in biological systems. Recent improvements in the theoretical treatment of *J*-couplings[5] have allowed accurate quantitative correlations to be established between *J*-coupling magnitude and molecular structure. In a detailed study[4d] of the structural dependence of interresidue $^{3h}J_{NC'}$ scalar couplings in α-helices and β-sheets in proteins, Barfield found that the magnitude of these *J*-couplings is explicitly dependent on the local geometry of the hydrogen bond (H-bond), in particular, the H···O internuclear separation, the C═O···H angle and the N−C═O···H dihedral angle. Despite the fact that the computed coupling constants for the 1.1 Å X-ray structure of protein G are in reasonable agreement with the experimental data, the discrepancy between theory and experiment is considerably larger than one would expect. We consider that this discrepancy arises from the fact that all studies performed to date are based on static structures and neglect the effects of conformational motion. There has been considerable work in establishing the effect of conformational averaging on measured observables associated with a distribution over an ensemble of microscopic states.[6] Recent simulations of proteins[7] have demonstrated that it is possible to obtain ensemble averages compatible with a particular microscopic state from the trajectory of a single molecule. In the present work, we combine molecular dynamics simulation with density functional theory (DFT)/finite perturbation theory (FPT) to obtain the Fermi contact contributions to $^{3h}J_{NC'}$ scalar couplings in the SMN Tudor domain. For this 55-residue β-barrel-shaped protein both a 1.8 Å resolution X-ray structure and a well-defined NMR structure are available.[8] Experimental $^{3h}J_{NC'}$ scalar couplings were measured as described.[3b] The observed *J*-couplings vary from 0.0 to −0.45 Hz with an estimated experimental error of 0.02 Hz.

To include the effects of conformational motion, we have performed a MD simulation using the AMBER program suite.[9] A generalized Born (GB) solvation model was used with a modified set of Bondi radii and screening parameters adopted from the Tinker programs.[10] Starting from the 1.8 Å resolution X-ray structure for the initial coordinate geometry, a short 20-ps conjugate gradients energy minimization was performed. The system was then slowly heated from 0 to 300 K over 50 ps with a time constant for heat-bath coupling of 0.2 ps. This was followed by another 50-ps MD run in which the coupling to the heat bath was slowly removed. After these equilibration procedures, a 500-ps MD run was performed with constant total energy dynamics using a 1-fs time-step. For all simulations a nonbonded electrostatic cutoff of 20 Å was employed, and no constraints were placed on the chemical bonds. Protein structures were saved every 0.5 ps during the simulation for the calculation of the $^{3h}J_{NC'}$ scalar couplings.

The dominant term in the *J*-coupling interaction is the Fermi contact (FC) contribution, which is very sensitive to the effects of exchange correlation.[5b] For this reason DFT methods are readily employed, particularly when studying large systems. In the DFT/FPT[11] formalism, the *J*-coupling is expressed in terms of the derivative of the spin density matrix elements, computed in the presence of a single hypothetical magnetic moment at a given nucleus A with respect to this magnetic moment. The wave function is perturbed by the presence of the magnetic moment at nucleus A which is represented by a Fermi contact perturbation of magnitude λ. As a result, couplings between the nucleus A and all other magnetic nuclei in the molecule are obtained in a single calculation. Using finite difference methods, the *J*-coupling between nucleus A and any other magnetic nucleus B in the system is given by:[5b]

$$J_{AB} = (\mu_0/4\pi)^2(h/4\pi^2)(8\pi\beta/3)^2 a_0^{-6}\gamma_A\gamma_B\lambda^{-1}\mathrm{FC}_{(B)}$$

where γ_I is the gyromagnetic ratio of nucleus I, β is the Bohr magneton, a_0 the Bohr radius, and $\mathrm{FC}_{(B)}$ is the Fermi contact coupling energy at nucleus B after the SCF (self-consistent field) calculation has been performed. At every 0.5-ps interval during the MD simulation, each $^{3h}J_{NC'}$ scalar coupling constant was calculated using DFT/FPT at the UB3LYP/6-311G** level of theory with a FC perturbation of magnitude $\lambda = 0.002$ au. As these *J*-couplings are only dependent on the local geometry of the system,[4d] molecular fragments containing just the two hydrogen-bonded residues were considered. The resulting *J*-couplings were then averaged over the 500-ps MD trajectory. All DFT calculations were performed using the Gaussian 98 program suite.[12]

The correlation between the experimental *J*-coupling data and the MD/DFT/FPT results is shown in Figure 1. We observe a dramatic improvement in the predicted *J*-couplings (average rmsd between theory and experiment 0.04 Hz) compared to the calculations performed using the static X-ray (rmsd 0.35 Hz) and the lowest-energy NMR (rmsd 0.19 Hz) structures. The principle source of uncertainty in the DFT calculations arises from errors in the wave function. We calculated several *J*-couplings using different functionals (B3PW91, BLYP) and found an average difference of 0.05 Hz, which we assume to be the associated theoretical error.

On analyzing the calculated $^{3h}J_{NC'}$ couplings over the MD trajectory, the cumulative *J*-coupling averages for H-bonds in the β-sheet regions remain ostensibly constant after the first 200 ps. In comparison, the cumulative $^{3h}J_{NC'}$ coupling averages associated with more flexible regions at the edges of the β-sheets vary over the 500-ps trajectory. This provides a qualitative insight into the degree of conformational freedom in different regions of the protein. In principle, one could progress to longer trajectories until the cumulative average for the *J*-couplings in these flexible regions also converges.

The results shown in Figure 1 require a large number of DFT calculations demanding extensive CPU time. However, from a practical point of view, it is important to note that the *J*-coupling

10.1021/ja028875w CCC: $25.00

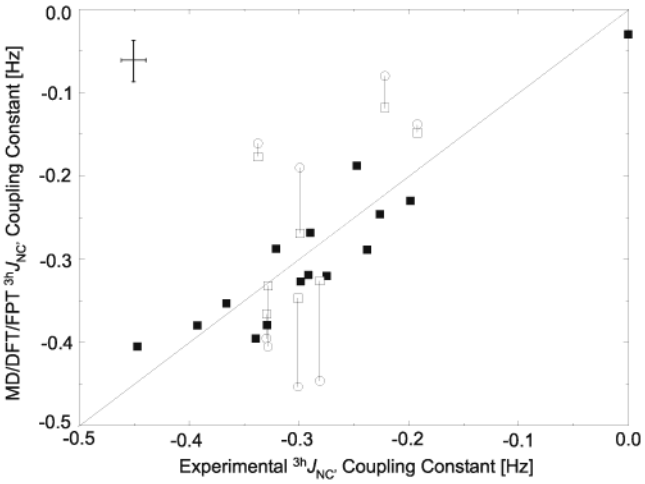

Figure 1. Correlation between experimental data and the MD/DFT/FPT results. The rms deviation is 0.04 Hz. The solid squares are *J*-couplings in the β-sheet regions averaged over a 200-ps trajectory. The open circles are *J*-couplings involving residues at the edges of the β-sheets averaged over a 200-ps trajectory. The open squares are *J*-couplings involving these residues averaged over a 500-ps trajectory. After 200 ps, the cumulative *J*-coupling averages in the β-sheet regions remain constant.

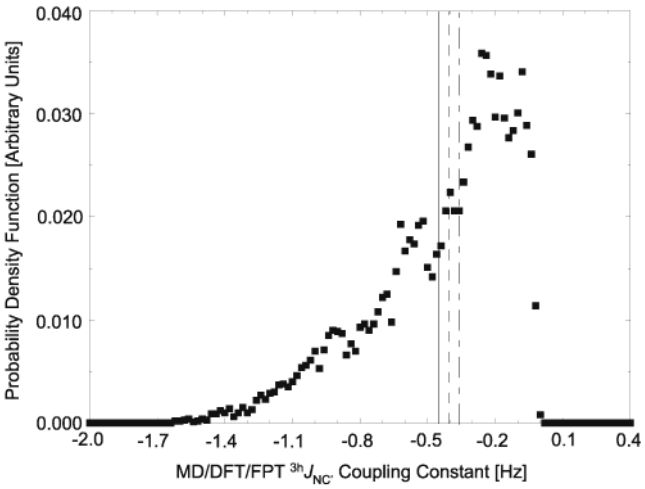

Figure 2. Distribution function for the *J*-coupling constant between Ala[36] (N) and Val[46] (C′) over the 500-ps MD trajectory. The solid line shows the experimental result (−0.45 Hz), the dashed line is the distribution average (−0.41 Hz), and the dot−dashed line shows the result obtained for the geometrical average over the 500-ps MD simulation (−0.38 Hz).

values calculated for the MD-averaged H-bond geometries are also in excellent agreement with the experimental data (rmsd 0.11 Hz) and are significantly better than the results obtained using static structures (rmsd 0.35 and 0.19 Hz) as shown in Figure 2.

Our results show that the effect of conformational motion plays a significant role in the accurate prediction of $^{3h}J_{NC'}$ scalar couplings. Figure 2 shows a representative skewed *J*-coupling distribution function. The *J*-coupling magnitude varies from 0 to −1.5 Hz, which demonstrates a considerable variation in the local molecular geometry about the H-bond. The probability distributions for both the average H-bond length and geometry are very similar to those obtained by M. Buck and M. Karplus.[13]

The variations over H-bond geometry observed in the MD are reflected in the dynamically averaged *J*-couplings. This suggests that the H-bond network which stabilizes the secondary structure is compatible with substantial conformational freedom in the peptide backbone. The backbone dynamics presumably reduces the entropy loss that is associated with H-bond formation and therefore stabilizes the folded conformation of a protein.[14] Our results indicate, that the inclusion of conformational motion is necessary for the accurate theoretical prediction of any physicochemical property which is dependent on local molecular geometry in the peptide backbone.

Acknowledgment. This work was supported by grants from the DFG and the EU (M.S.). P.M. acknowledges an EMBO-Fellowship. We thank M. Nilges for discussions and support.

Supporting Information Available: Calculated and experimental *J*-couplings, energy fluctuations, and H-bond statistics for the MD trajectory (PDF). This material is available free of charge via the Internet at http://pubs.acs.org.

References

(1) Jeffrey, G. A.; Saenger, W. *Hydrogen Bonding in Biological Structures*; Springer: New York, 1991.
(2) Dingley, A. J.; Grzesiek, S. *J. Am. Chem. Soc.* **1998**, *120*, 8293−8297.
(3) (a) Pervushin, K.; Ono, A.; Fernandez, C.; Szyperski, T.; Kainosho, M.; Wüthrich, K. *Proc. Natl. Acad. Sci. U.S.A.* **1998**, *95*, 14147−14151. (b) Cordier, F.; Grzesiek, S. *J. Am. Chem. Soc.* **1999**, *121*, 1601−1602. (c) Cornilescu, G.; Hu, J.-S.; Bax, A. *J. Am. Chem. Soc.* **1999**, *121*, 2949−2950. (d) Cornilescu, G.; Ramirez, B. E.; Frank, M. K.; Clore, G. M.; Gronenborn, A. M.; Bax, A. *J. Am. Chem. Soc.* **1999**, *121*, 6275−6279. (e) Juranić, N,; Macura, S. *J. Am. Chem. Soc.* **2001**, *123*, 4099−4100.
(4) (a) Scheuer, C.; Brüschweiler, R. *J. Am. Chem. Soc.* **1999**, *121*, 8661−8662. (b) Bagno, A. *Chem Eur. J.* **2000**, *6*, 2925−2930. (c) Czernek, J.; Brüschweiler, R. *J. Am. Chem. Soc.* **2001**, *123*, 11079−11080. (d) Barfield, M. *J. Am. Chem. Soc.* **2002**, *124*, 4158−4168.
(5) (a) Carmichael, I. *J. Phys. Chem.* **1993**, *97*, 1789−1792. (b) Malkin, V. G.; Malkina, O. L.; Salahub, D. R. *Chem Phys. Lett.* **1994**, *221*, 91−99. (c) Hricovini, M.; Malkina, O. L.; Bizik, F.; Nagy, L. T.; Malkin, V. G. *J. Phys. Chem. A* **1997**, *101*, 9756−9762.
(6) (a) Bürgi, R.; Pitera, J.; van Gunsteren, W. F. *J. Biomol. NMR* **2001**, *19*, 305−320 and references therein. (b) Case, D. A.; Scheurer, C.; Brüschweiler, R. *J. Am. Chem. Soc.* **2000**, *122*, 10390−10397. (c) Hoch, J. C.; Dobson, C. M.; Karplus, M. *Biochemistry* **1985**, *24*, 3831−3841.
(7) Daura, X.; Antes, I.; van Gunsteren, W. F. Thiel, W.; Mark, A. *Proteins* **1999**, *36*, 542−555.
(8) (a) Selenko, P.; Sprangers, R.; Stier, G.; Bühler, D.; Fischer, U.; Sattler, M. *Nat. Struct. Biol.* **2001**, *8*, 27−31. (b) Sprangers, R.; Groves, M.; Sinning, I.; Sattler, M. Manuscript submitted.
(9) Case, D. A.; Pearlman, D. A.; Caldwell, T. W.; Cheatham, T. E., III; Ross, W. S.; Simmerling, C. L.; Darden, T. A.; Marz, K. M.; Stanton, R. V.; Cheng, A. L.; Vincent, J. J.; Crowley, M.; Tsui, V.; Radmer, R. J.; Duan, Y.; Pitera, J.; Massova, I.; Seibel, G. L.; Singh, U. C.; Weiner, P. K.; Kollman, P. A. *AMBER 6*; University of California: San Fransisco, 1999.
(10) Tsui, V.; Case, D. A. *J. Am. Chem. Soc.* **2000**, *122*, 2489−2498.
(11) Pople, J. A.; McIver, J. W., Jr.; Ostlund, N. S. *J. Chem. Phys.* **1968**, *49*, 2960−2964 and 2965−2970.
(12) Frisch, M. J.; Trucks, G. W.; Schlegel, H. B.; Scuseria, G. E.; Robb, M. A.; Cheeseman, J. R.; Zakrzewski, V. G.; Montgomery, J. A., Jr.; Stratmann, R. E.; Burant, J. C.; Dapprich, S.; Millam, J. M.; Daniels, A. D.; Kudin, K. N.; Strain, M. C.; Farkas, O.; Tomasi, J.; Barone, V.; Cossi, M.; Cammi, R.; Mennucci, B.; Pornelli, C.; Adamo, C.; Clifford, S.; Ochterski, J.; Petersson, G. A.; Ayala, P. Y.; Cui, Q.; Morokuma, K.; Salvador, P.; Dannenberg, J. J.; Malick, D. K.; Rabuck, A. D.; Raghavachari, Foresman, J. B.; Cioslowski, J., Ortiz, J. V.; Baboul, A. G.; Stefanov, B. B.; Liu, G.; Liashenko, A.; Piskorz, P.; Komaromi, I.; Gomperts, R.; Martin, R. L.; Fox, D. J.; Keith, T.; Al-Laham, A.; Peng, C. Y.; Nanayakkara, A.; Challacombe, M.; Gill, P. M. W.; Johnson, B.; Chen, W.; Wong, M. W.; Andres, J. L.; Gonzalez, C.; Head-Gordon, M.; Replogle, E. S.; Pople, J. A. *GAUSSIAN 98*, rev. A.11; Gaussian Inc.: Pittsburgh, PA, 2001.
(13) Buck, M.; Karplus, M. *J. Phys. Chem. B.* **2001**, *105*, 11000−11015.
(14) Schafer, H.; Duara, X.; Mark, A. E.; van Gunsteren, W. F. *Proteins* **2001**, *43*, 45−56.

JA028875W